Dimensional Reduction for 6D Vibrotactile Display

Ruisi Zhang, *Student Member, IEEE*, Trevor J. Schwehr, and Jake J. Abbott, *Senior Member, IEEE*

***Abstract*—The human hand detects high-frequency vibrations in all directions but cannot distinguish the direction, which suggests a multi-dimensional vibrotactile stimulus is haptically equivalent to some one-dimensional (1D) stimulus. In this article, we explore how a 6D vibrotactile stimulus rendered at the haptic interaction point (HIP) of a kinesthetic haptic interface, with the stylus held in a precision pen-hold grasp, is mapped to an equivalent 1D stimulus normalized by the detection threshold. We gather a large human-subjects data set in which we determine detection thresholds for 45 distinct combinations of three orthogonal forces and three orthogonal torques rendered at the HIP, at a single frequency of 108 Hz corresponding to the peak sensitivity in our prior study. Using this data set, we find a general quadratic weighting function to predict the 1D normalized stimulus for a given 6D vibrotactile stimulus. We find that including just seven (out of a possible 21) independent parameters in the symmetric weighting matrix is sufficient to capture the non-obvious coupling between forces and torques rendered at the HIP for dimensional reduction from 6D to 1D.**

***Index Terms*—Tool-mediated vibrotactile perception, high-frequency vibrations, pen-hold grasp, untethered magnetic haptic interface.**

I. Introduction

When humans haptically interact with objects, they use high-frequency vibrations, sensed in cutaneous mechanoreceptors in the skin, to identify the object's texture [1]–[3], and to inform estimates of other material properties at the contact event [4], [5]. Of particular interest is vibrotactile perception when using a pen-like stylus with a precision grasp (Fig. 1); the precision grasp is commonly used to manipulate a tool [6], and stylus-based haptic devices are commonly available commercially [7].

The human hand detects high-frequency vibrations in all directions but cannot distinguish the direction [8], which suggests a multi-dimensional vibrotactile stimulus is haptically equivalent to some one-dimensional (1D) stimulus. In haptic rendering, we have the opportunity to create the illusion of a given stimulus at a given frequency by providing a different stimulus that will be perceived as having the same intensity. There are two approaches to provide a vibrotactile stimulus using stylus-based kinesthetic haptic interfaces: one is to attach one or more auxiliary vibrotactile actuators [7], [9], and the other is to use the haptic device's native actuators [4], [10]. Stylus-based kinesthetic haptic interfaces can render up to 6D vibrotactile stimuli—typically either 3D, 5D, or 6D—at the haptic interaction point (HIP). However, we currently lack the understanding of how a 6D stimulus is dimensionally reduced to a 1D stimulus.

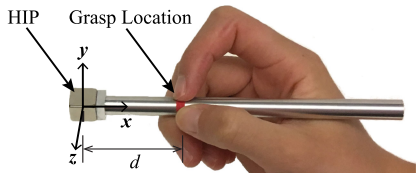

Fig. 1. Posture of a precision grasp, shown with the stylus of the untethered magnetic haptic interface used in this study. Forces and torques are applied at the haptic interaction point (HIP). The coordinate system used defines x along the stylus, y pointing upward, and z pointing toward the subject when the stylus is held in front of the subject. The HIP and grasp location are separated by distance d.

Previous studies considered how a 3D force-driven vibrotactile stimulus maps to an equivalent 1D stimulus that can be rendered by one or more vibrotactile actuators [11], [12]. They considered three orthogonal high-frequency accelerations (rather than forces), each characterized by a magnitude and a phase. However, forces and accelerations are highly correlated, and under certain assumptions are proportional. They reported that their discrete Fourier transform DFT321 (read as "DFT 3 to 1") method is the best method found to date for both offline and real-time dimensional reduction. DFT321 calculates the root-sum-of-squares (i.e., 2-norm) of the magnitudes and the sum of phases, for the three components of a stimulus signal in frequency domain, and then transfers the dimensionally reduced signal to time domain using an inverse discrete Fourier transform function, which accurately captures the mapping from 3D to 1D.

It is unclear if and how the DFT321 method can be extended to the general 6D problem, for a variety of reasons. First, torques and forces have different units, so combining them with a single 2-norm is not meaningful. Second, forces applied in three orthogonal directions at the HIP also result in orthogonal motions (or reaction forces and torques) at the grasp location, but the same cannot be said for forces and torques applied in six orthogonal directions at the HIP. Third, our prior study [13] found that subjects had comparable sensitivity to all three principal force directions at most frequencies, which is largely in agreement with the assumptions of DFT321, but a substantially different result was found when comparing the three principal torque directions (with high sensitivity to the stylus-axis torque).

In this article, we explore how a 6D vibrotactile stimulus rendered at the HIP is mapped to an equivalent 1D stimulus

Manuscript received September 28, 2019; revised December 30, 2019; accepted January 8, 2020. Date of publication January 12, 2020; date of current version March 17, 2020. This work was supported by the National Science Foundation under Grant 1423273. This article was recommended for publication by Associate Editor M. Wiertlewski and Editor Lynette Jones upon evaluation of the reviewers' comments. *(Corresponding author: Ruisi Zhang.)*

The authors are with the Department of Mechanical Engineering and the Robotics Center, University of Utah, Salt Lake City UT 84112 USA (e-mail: ruisi.zhang@utah.edu; trevor.schwehr@utah.edu; jake.abbott@utah.edu).

Digital Object Identifier 10.1109/TOH.2020.2966483

normalized by the detection threshold, based on a large human-subjects data set (Section II), using an energy-preserving method (Section III). We consider a 6D vibrotactile stimulus comprising six orthogonal sinusoidal signals at the HIP that are perfectly in phase but with arbitrary (including negative) magnitudes. We consider the stimulus detection threshold, using a single stylus with a precision grasp, at a single frequency (108 Hz) corresponding to the peak sensitivity in our prior study [13].

In this study, we make use of an untethered magnetic haptic interface (UMHI) comprising an electromagnetic field source and a fully untethered stylus with a permanent magnet at the HIP (Figs. 1 and 2). A UMHI is fundamentally like any other impedance-type haptic interface [14], in that actuator currents are mapped to configuration-dependent forces and torques at the HIP [15]. However, a UMHI enables application of pure forces and torques at the HIP without any directionally dependent confounding factors of device inertia (which are known to affect vibrotactile sensations [2], [16]) that may be present with a linkage-based haptic device.

II. Generating a Data Set of 6D Detection Thresholds

In this section, we generate a large data set of detection threshold values for 6D vibrotactile stimuli.

A. Subjects

The psychophysical study was performed by six male and six female subjects, ages 19–31, who are student volunteers that gave informed consent. Subjects have normal tactile sensation and normal (corrected) vision, by self-report. The study was approved by the University of Utah Institutional Review Board (IRB #00096461).

B. Apparatus

To render vibrotactile stimuli, we use an untethered magnetic haptic interface comprising an electromagnetic field source known as an Omnimagnet and a fully untethered stylus that has a cubic permanent magnet attached at one end, the center of which serves as the HIP (Figs. 1 and 2). An Omnimagnet [17] comprises three mutually orthogonal nested coils with a spherical ferromagnetic core in the center, with a design that was optimized to maximize the accuracy of the dipole field model as a description of its field:

$$\boldsymbol{b}(\boldsymbol{p}) = \frac{\mu_0}{4\pi\|\boldsymbol{p}\|^5}\left(3\boldsymbol{p}\boldsymbol{p}^T - \|\boldsymbol{p}\|^2 I\right)\boldsymbol{M} \tag{1}$$

where $\boldsymbol{M}$ (units A·m^2) is the dipole moment of the Omnimagnet, $\boldsymbol{p}$ (units m) is a vector from the center of the Omnimagnet (i.e., the location of the dipole moment) to the point where the magnetic field vector $\boldsymbol{b}$ (units T) is measured, $\mu_0 = 4\pi \times 10^{-7}$ T·m·A^{-1} is the permeability of free space, and I is the identity matrix. We utilize the middle and outer coils of the Omnimagnet, with a dipole strength proportional to coil currents (packed in array $\boldsymbol{i}$ (units A) as $\boldsymbol{M} = 6.87\boldsymbol{i}$ A·m^2. We characterized the frequency response of each coil using a Hewlett Packard dynamic signal analyzer (model 35665 A). The frequency response of each of the middle and outer coils in the range of 6–1000 Hz is accurately modeled as a first-order RL circuit. At 108 Hz, the gain of the middle and outer coil are 0.0164 A/V and 0.0160 A/V, respectively. The two coils are powered by a two-channel class D audio amplifier (Crown, model XLS 2002), capable of 1050 W of maximum output power for frequencies of 20 Hz to 20 kHz. The frequency response of the amplifier connected to (i.e., loaded by) the coil was measured by a dynamic signal analyzer. The amplifier's gain is 49.1 at 108 Hz. The amplifier outputs a high-power sinusoidal voltage to the coil, given a low-power sinusoidal voltage (i.e., audio signal) from a computer running a MATLAB program, which is generated by an onboard Realtek sound card (model ALC 887). The gain between the commanded MATLAB signal and the measured output voltage from the sound card is 2.44 at 108 Hz. All commanded vibrotactile signals in this study are well below the saturation limit of the system.

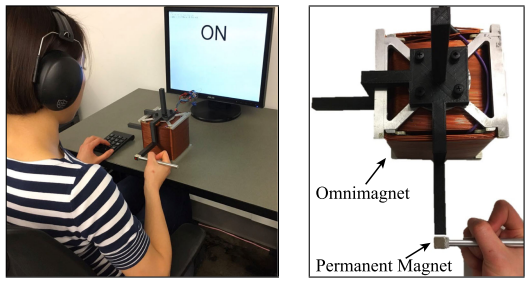

Fig. 2. (Left) Experimental setup. The subject holds the stylus with a precision grasp, with the black mark on the magnet (shown red here for clarity) facing the subject, and with their forearm resting on an armrest. (Right) Close-up showing the untethered magnetic haptic interface. The subject places the stylus's permanent magnet at a location indicated by a given nonmagnetic rod extending from the Omnimagnet, without contacting it.

The magnetic field from the electromagnet generates a force $\boldsymbol{f} = \nabla(\boldsymbol{m}\cdot\boldsymbol{b})$ (units N) and torque $\boldsymbol{\tau} = \boldsymbol{m}\times\boldsymbol{b}$ (units N·m) on the stylus's magnetic dipole $\boldsymbol{m}$ (units A·m^2) [15], which can be modeled as being at the center of the cubic NdFeB permanent magnet with dipole strength $\|\boldsymbol{m}\| = 2.15$ A·m^2 and mass $m_m = 15.4$ g. The aluminum stylus has mass $m_s = 25.8$ g, diameter $D = 9.53$ mm, and length $L_s = 131$ mm. The stylus with the attached permanent magnet has inertia $I_{xx} = 0.724$ kg·mm^2, $I_{yy} = I_{zz} = 86.4$ kg·mm^2. The black mark on one of faces of the permanent magnet indicates the desired orientation of the stylus such that the marked face is facing the subject (Fig. 2). The red band on the stylus indicates the desired resting position (i.e., grasp location) of the stylus on the subject's middle finger (Fig. 1). The stylus was designed such that its center of mass (including the permanent magnet) is located at the grasp location, such that it feels balanced. The effective distance between the HIP and the grasp location is $d = 44.1$ mm.

C. Design

We consider 45 configurations of vibrotactile stimulus (Fig. 3): six correspond to a single component, 18 correspond to two components, 18 correspond to three components, and three correspond to four components. These 45 configurations represent all possible distinct combinations that we can render

Comp.	Conf.	Pose	$\boldsymbol{i}$ (A)			$\frac{\boldsymbol{m}}{2.15}$ (A·m^2)			$\frac{\boldsymbol{p}}{0.16}$ (m)			$\boldsymbol{f}$ (mN)			$\boldsymbol{\tau}$ (mN·m)		
			x	y	z	x	y	z	x	y	z	x	y	z	x	y	z
1	1	b-1	-	i	-	-	1	-	1	-	-	$6.1i$	-	-	-	-	-
	2	c-2	-	-	i	-	-	1	-	1	-	-	$6.1i$	-	-	-	-
	3	a-3	i	-	-	1	-	-	-	-	1	-	-	$6.1i$	-	-	-
	4	b-1	-	i	-	-	-	1	1	-	-	-	-	-	$0.33i$	-	-
	5	c-2	-	-	i	1	-	-	-	1	-	-	-	-	-	$0.33i$	-
	6	a-3	i	-	-	-	1	-	-	-	1	-	-	-	-	-	$0.33i$
2	7	c-1	-	i	i	-	-	1	1	-	-	$6.1i$	-	-	$0.33i$	-	-
	8	c-1	-	i	i	-	1	-	1	-	-	$6.1i$	-	-	$-0.33i$	-	-
	9	a-2	i	-	i	1	-	-	-	1	-	-	$6.1i$	-	-	$0.33i$	-
	10	a-2	i	-	i	-	-	1	-	1	-	-	$6.1i$	-	-	$-0.33i$	-
	11	b-3	i	i	-	-	1	-	-	-	1	-	-	$6.1i$	-	-	$0.33i$
	12	b-3	i	i	-	1	-	-	-	-	1	-	-	$6.1i$	-	-	$-0.33i$
	13	a-3	i	-	-	-	-	1	-	-	1	$6.1i$	-	-	-	$-0.33i$	-
	14	c-3	-	-	i	1	-	-	-	-	1	$6.1i$	-	-	-	$-0.67i$	-
	15	a-2	i	-	-	-	1	-	-	1	-	$6.1i$	-	-	-	-	$0.33i$
	16	b-2	-	i	-	1	-	-	-	1	-	$6.1i$	-	-	-	-	$0.67i$
	17	b-3	-	i	-	-	-	1	-	-	1	-	$6.1i$	-	$0.33i$	-	-
	18	c-3	-	-	i	-	1	-	-	-	1	-	$6.1i$	-	$0.67i$	-	-
	19	c-2	-	-	i	-	1	-	-	1	-	-	-	$6.1i$	$-0.33i$	-	-
	20	b-2	-	i	-	-	-	1	-	1	-	-	-	$6.1i$	$-0.67i$	-	-
	21	c-1	-	-	i	1	-	-	1	-	-	-	-	$6.1i$	-	$0.33i$	-
	22	a-1	i	-	-	-	-	1	1	-	-	-	-	$6.1i$	-	$0.67i$	-
	23	b-1	-	i	-	1	-	-	1	-	-	-	$6.1i$	-	-	-	$-0.33i$
	24	a-1	i	-	-	-	1	-	1	-	-	-	$6.1i$	-	-	-	$-0.67i$
3	25	b-1	i	i	-	-	1	-	1	-	-	$6.1i$	$6.1i$	-	-	-	$-0.67i$
	26	b-2	i	i	-	1	-	-	-	1	-	$6.1i$	$6.1i$	-	-	-	$0.67i$
	27	a-1	i	-	i	-	-	1	1	-	-	$6.1i$	-	$6.1i$	-	$0.67i$	-
	28	a-3	i	-	i	1	-	-	-	-	1	$6.1i$	-	$6.1i$	-	$-0.67i$	-
	29	b-1	i	i	-	1	-	-	1	-	-	$-12i$	$6.1i$	-	-	-	$-0.33i$
	30	b-2	i	i	-	-	1	-	-	1	-	$6.1i$	$-12i$	-	-	-	$0.33i$
	31	a-1	i	-	i	1	-	-	1	-	-	$-12i$	-	$6.1i$	-	$0.33i$	-
	32	a-3	i	-	i	-	-	1	-	-	1	$6.1i$	-	$-12i$	-	$-0.33i$	-
	33	c-2	-	i	i	-	1	-	-	1	-	-	$-12i$	$6.1i$	$-0.33i$	-	-
	34	c-3	-	i	i	-	1	-	-	-	1	-	$6.1i$	$6.1i$	$0.67i$	-	-
	35	c-2	-	i	i	-	-	1	-	1	-	-	$6.1i$	$6.1i$	$-0.67i$	-	-
	36	c-3	-	i	i	-	-	1	-	-	1	-	$6.1i$	$-12i$	$0.33i$	-	-
	37	c-2	-	i	i	1	-	-	-	1	-	$6.1i$	-	-	-	$0.33i$	$0.67i$
	38	c-3	-	i	i	1	-	-	-	-	1	$6.1i$	-	-	-	$-0.67i$	$-0.33i$
	39	a-1	i	-	i	-	1	-	1	-	-	-	$6.1i$	-	$-0.33i$	-	$-0.67i$
	40	a-3	i	-	i	-	1	-	-	-	1	-	$6.1i$	-	$0.63i$	-	$0.33i$
	41	b-1	i	i	-	-	-	1	1	-	-	-	-	$6.1i$	$0.33i$	$0.67i$	-
	42	b-2	i	i	-	-	-	1	-	1	-	-	-	$6.1i$	$-0.67i$	$-0.33i$	-
4	43	b-3	i	i	-	-	-	1	-	-	1	$6.1i$	$6.1i$	-	$0.33i$	$-0.33i$	-
	44	a-2	i	-	i	-	1	-	-	1	-	$6.1i$	-	$6.1i$	$-0.33i$	-	$0.33i$
	45	c-1	-	i	i	1	-	-	1	-	-	-	$6.1i$	$6.1i$	-	$0.33i$	$-0.33i$

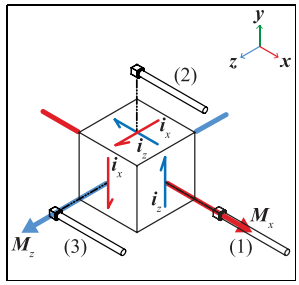

Pose (a)

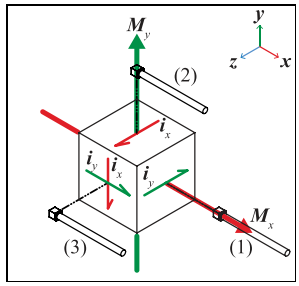

Pose (b)

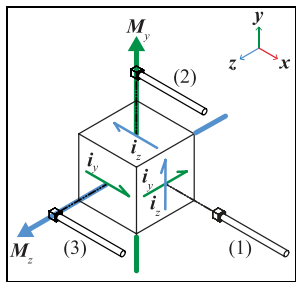

Pose (c)

Fig. 3. Parameters for the 45 configurations considered in the psychophysical study. The configurations are grouped by those comprised of one, two, three, or four principal components of vibrotactile stimulus. i represents the amplitude (i.e., half peak-to-peak) of the sinusoidal current, which is varied during the study to determine the detection threshold. The amplitudes of the resulting sinusoidal force and torque, which are proportional to i, are provided. The nine different poses used are also depicted. Each of poses (a)–(c) corresponds to a unique orientation of the Omnimagnet; when current i flows through the middle and/or outer coil of the Omnimagnet, they generate the corresponding dipole moment $\boldsymbol{M}$, located at the Omnimagnet's center. At each of the nine poses, the stylus's magnetic dipole $\boldsymbol{m}$ can also be rotated.

with the stylus held in the same orientation, and with either one coil or two coils being activated simultaneously using the same sinusoidal current signal. We render these 45 configurations by manipulating the orientation of the Omnimagnet for the desired $\boldsymbol{i}$, the orientation of the permanent magnet for the desired $\boldsymbol{m}$, and the position of the stylus for the desired $\boldsymbol{p}$.

We are interested in determining the detection threshold of the intensity (i.e., half peak-to-peak amplitude) of the vibrotactile stimulus at a given frequency that can be perceived for each configuration. This is done first in terms of the sinusoidal current signal, which is then converted into intensity of the respective force and torque stimuli at the HIP, using the formulas provided in the table of Fig. 3.

D. Procedure

The experiment was conducted in three sessions, each considering a single Omnimagnet orientation (Poses (a)–(c) in Fig. 3) and lasting 15–30 minutes per subject (the subject was allowed to take a break at any time). The sessions were separated by at least 48 hours to mitigate the effect of the configuration order [18]. The order of the sessions was randomized for each subject to mitigate the effect of learning and fatigue. Each session comprised 15 distinct configurations, with the order randomized for each subject.

In each session, the subject sat in front of the table with the Omnimagnet on it (Fig. 2). The 100-mm-long rectangular nonmagnetic rod attached to a given side of the Omnimagnet

indicated the desired position of the stylus. The subject was instructed to rest their forearm on the armrest, hold the stylus using a precision grasp—with the center of the middle finger contacting the red band, and with the black mark on the magnet facing the subject—and place the center of the stylus's permanent magnet very close to the end of a given rod without contacting it. The experimenter changed the location and/or orientation of the permanent magnet (including removal and reattachment to the stylus, using beeswax) up to eight times during each session. For each new pose, the subject was instructed to adjust the height of the chair, the height of the armrest, and the position of the Omnimagnet on the table to facilitate a comfortable and consistent precision grasp on the stylus. With these adjustments, the subject was able to hold the stylus in the same orientation with the same wrist posture, relative to the armrest, for all 45 configurations. A 508 mm (20 inch) monitor, placed at an approximate distance of 700 mm from the subject, provided a visual display. The subject wore ear muffs for the duration of the experiment to eliminate the potential audio cues from the device and other distractions. The subject was given no information about the vibration parameters.

A staircase method was used to determine the best estimate threshold (BET) for a given configuration [19], [20]. Each stimulus was displayed for 1 s, during which the text "ON" was simultaneously displayed on the monitor (Fig. 2 (Left)). There was no text displayed on the monitor between stimuli. Each trial forced the subject to answer whether or not they could perceive the stimulus. There was a pause after each stimulus to allow the subject to manually input their answer on a numeric keypad ("1" for yes and "0" for no), after which the next trial began automatically. For each staircase (i.e., each configuration), the intensity was started at a high value that is easily felt (determined during pilot testing among the authors) without being excessively high, decreased after any correct response, increased after any incorrect response, and finally stopped after completing the 13^{th} trial. The initial step size (from trial 1 to trial 2) is half of the initial intensity. The step size is then successively divided by 2 for the transitions from trial 2 to trial 3 and from trial 3 to trial 4, and the step size then remains constant for the remaining trials. There is no stimulus in the seventh trial, in order to check for the existence of a false alarm. If the subject answered "yes" for this trial, the staircase procedure started over for this configuration. If the subject answered "no" for this trial, as is typical, the staircase procedure continued, in which the answer from trial 6 was used to determine the intensity of trial 8. The BET for each configuration was computed as the median intensity of all trials except trial 7 (i.e., the trial with no stimulus).

III. 6-to-1 Dimensional Reduction

In this section, we propose an effective dimensional-reduction method to reduce a 6D vibrotactile stimulus, corresponding to the six principal components $\{f_x, f_y, f_z, \tau_x, \tau_y, \tau_z\}$ applied at the HIP, to an equivalent 1D stimulus. In this article, we consider only the detection threshold of vibrotactile perception at the frequency of 108 Hz without phase shifting between principal components, which were determined in the psychophysical study of Section II.

Hwang *et al.* [21] suggested to use a 1D skin-absorbed power function $P_A(f) = \mathrm{Re}\{(Z(f)\}(A(f)/(2\pi f))^2$ as a physical metric for perceived intensity at a given frequency, where $Z(f)$ is the mechanical impedance that describes the biomechanical property of the hand-arm system, which is approximately constant at frequencies above 60 Hz, and $A(f)$ is the magnitude of the Fourier transform of the input acceleration signals at a given frequency f. However, this work considered only the three orthogonal forcing directions (i.e., x, y, and z) independently (i.e., one at a time).

For a 3D force-driven vibrotactile stimulus, previous works suggested humans are perceiving the total energy spectral density (ESD) of the acceleration signal [11], [12], which is calculated over all frequencies in the range of 20–1000 Hz for all three principal components: $\mathrm{ESD} = \sum_f (A_x(f)^2 + A_y(f)^2 + A_z(f)^2)$. This DFT321 method relies on an assumption of orthogonality (in terms of vibrotactile sensation) between the three orthogonal forcing directions.

We propose an energy-preserving method to capture the vibrotactile stimulus intensity at each frequency component for a 6D vibrotactile stimulus using a 1D stimulus signal $\tilde{P}(f)$, where $\tilde{P}$ is the normalized stimulus intensity determined by the Fourier transform at a given frequency f. We attempt to use $\tilde{P}$ to present the normalized skin-absorbed power (i.e., the skin-absorbed power divided by the skin-absorbed power at the detection threshold), since the skin-absorbed power can be further related to the perceived sensation magnitude, and ESD and skin-absorbed power are proportional at a given frequency. One benefit of normalizing the skin-absorbed power is the constant $\mathrm{Re}\{(Z(f)\}/(2\pi f)^2$ that has been considered in the skin-absorbed power equation will be canceled, so the impedance need not be known. There is another benefit of normalization. Howe and Cutkosky [22] suggest that humans sense accelerations in response to vibrotactile stimuli, and the skin-absorbed power function and DFT321 method are also formulated in terms of accelerations, whereas in our study stimuli are formulated in terms of forces and torques. If we consider that there is an admittance (i.e., inverse of impedance) between a given force-torque and the resulting acceleration due to the mechanical properties of the tool and hand, and we evaluate the admittance (in terms of transfer function) at a given frequency, we expect a proportionality constant between the force-torque intensity and the resulting acceleration intensity. During the process of normalization, that constant is also canceled, such that the results will be invariant to the formulation (i.e., force-torque vs. acceleration) used.

We note that although the six principal components of stimulus are orthogonal at the HIP, they are not orthogonal at the grasp location. It has also been shown that vibrotactile sensation is substantially affected by the specific precision grasp used [23]. We consider precision grasp holistically using a weighting function for each of the six principal components and the coupling between each of them, without any preconceived assumption of the orthogonality among the three orthogonal force directions and the three orthogonal torque directions at the HIP. Inspired

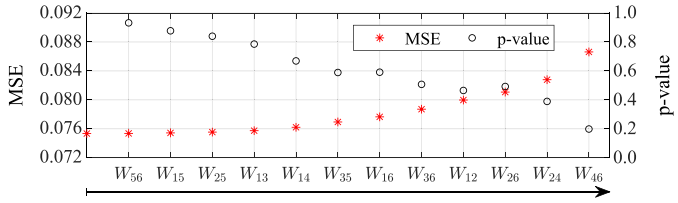

Fig. 4. Process for eliminating nonsignificant off-diagonal elements of W. From left to right, the element W_{ij} with the highest p-value (black circle) is shown, along with the MSE (red asterisk) that results after that element is eliminated from the model. This process is stopped after eliminating element W_{46}, at which point the remaining three off-diagonal terms all have $p < 0.1$.

Algorithm 1. Constructing the A matrix for (3)

```
for i ← 1 to n do
    v ← [f_xi f_yi f_zi τ_xi τ_yi τ_zi]^T
    V ← vv^T
    j ← 0
    for k ← 1 to 6 do
        for l ← k to 6 do
            j ← j + 1
            if l = k then
                A(i, j) ← V(k, l)
            else
                A(i, j) ← 2V(k, l)
            end if
        end for
    end for
end for
```

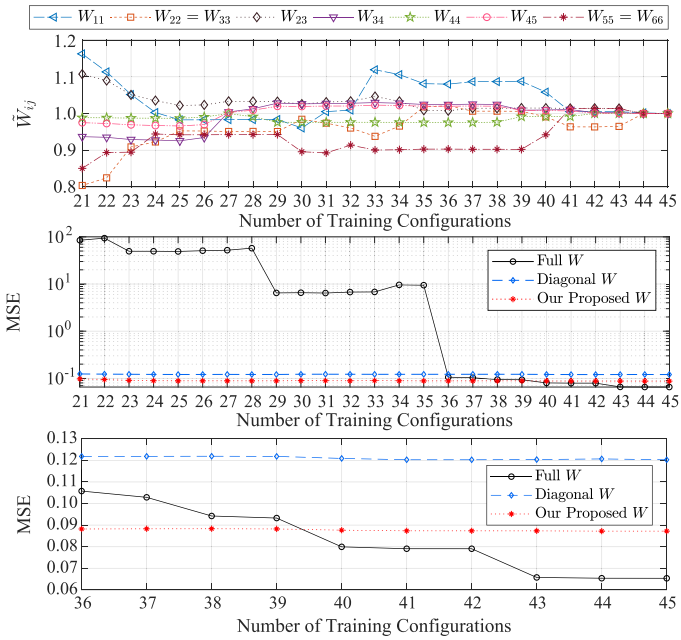

Fig. 5. (Upper) Normalized parameters ($\tilde{W}_{ij} = W_{ij,n}/W_{ij,n=45}$) of our proposed seven-term weighting matrix vs. number of training configurations n. (Middle) MSE vs. n, with a log-base-10 scale used in the ordinate due to the large range in MSE values observed at low n values. Curves are shown for the full 19-parameter W matrix, a three-parameter diagonal W matrix, and our proposed seven-parameter W matrix. (Lower) Zoomed version of MSE vs. n for high n.

$$A\begin{bmatrix} W_{11} & \cdots & W_{16} & W_{22} & \cdots & W_{26} & \cdots\cdots & W_{66} \end{bmatrix}^T = 1_{n\times 1} \tag{3}$$

by the previous studies discussed above, power could be described by each of the force principal components using a quadratic form. A general quadratic weighting function of the form

$$\tilde{P} = \begin{bmatrix} f_x & f_y & f_z & \tau_x & \tau_y & \tau_z \end{bmatrix} W \begin{bmatrix} f_x & f_y & f_z & \tau_x & \tau_y & \tau_z \end{bmatrix}^T \tag{2}$$

seems to embody the dimensional reduction that we are seeking, where W is a 6×6 symmetric weight matrix and $[f_x\ f_y\ f_z\ \tau_x\ \tau_y\ \tau_z]^T$ is the Fourier transform of the 6D vibrotactile stimulus at a given frequency (here 108 Hz, since we consider sinusoidal signals at a single frequency). The elements in W serve a dual purpose of normalizing the stimulus values and describing the coupling between the six orthogonal principal components at the HIP. The normalized skin-absorbed power with an ideal W would have an expected value of $\tilde{P} = 1$ for any given 6D stimulus at the detection threshold.

There are 21 independent elements W_{ij} in W due to symmetry, which we can estimate by using a linear least-squares regression approach with the experimental data gathered in Section II. We chose to use the median BET (across all subjects) for each of the configurations as our training data set, since a median of a data set is robust to its outliers and transformations (since we expect stimulus intensity to be logarithmic with skin-absorbed power based on Stevens' power law [24]). In general, we can choose any $n \geq 21$ of these data to estimate W. We set $\tilde{P} = 1$ in (2) for each of the n training configurations. These n equations can be manipulated into the form

where A is an $n \times 21$ matrix that is constructed as described in Algorithm 1, and $1_{n\times 1}$ in an $n \times 1$ all-ones vector. This system of equations is then solved numerically using a generalized inverse to obtain the best estimates of the elements of W with n training data.

Regardless of the value of n, the performance of a given W is evaluated using the mean square error calculated as $MSE = (1/45)\ \sum_{i=1}^{45} (\tilde{P} - 1)^2$ for entire training data set (45 median BETs) applied to (2).

We are interested in finding the simplest model that accurately predicts the 6D-to-1D mapping. We know that each of the diagonal elements in W is meaningful, since they correspond to the six individual principal components at the HIP. Our prior study [13] found that $W_{22} = W_{33}$ and $W_{55} = W_{66}$, which we use as two constrains in the linear least-squares regression approach. To evaluate the importance of each of the off-diagonal elements of W, which quantify the coupling between the principal modes, we use the p-value from the linear least-squares regression with $n = 45$, with the null hypothesis being that the off-diagonal element could be replaced with zero. We chose to use a significance of $\alpha = 0.1$. We begin with the full matrix W with 19 independent elements and then eliminate the off-diagonal element with the highest p-value from (3). After each elimination, we repeat the linear least-squares regression process using (3) to update the p-values, and we repeat until all elements are significant. Figure 4 shows the results for this process. Beginning with element W_{56},

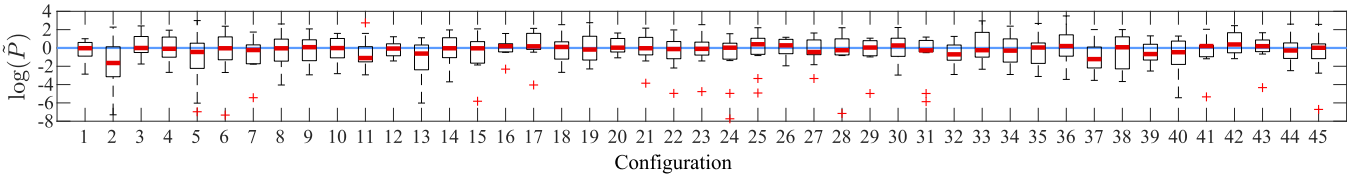

Fig. 6. Box-whisker plot showing estimated normalized skin-absorbed power in a log-base-10 scale using our proposed seven-parameter W, for all configurations and subjects tested (at 108 Hz). A perfect model would result in an estimated value of 0 (indicated with a blue line).

elements are eliminated one by one. With each element eliminated, the MSE grows from the 0.076 full-model baseline (as expected), but it grows slowly, which indicates that the model's predicting power is not substantially harmed by elimination of the element. After eliminating 12 elements with $p > 0.1$, only three off-diagonal elements remain (W_{23}, W_{45}, and W_{34}). These are combined with the six diagonal elements to form our proposed W.

The linear regression method has a potential to introduce a bias into the model, due to the fact that Steven's power law suggests that power maps to stimulus intensity logarithmically, not linearly [24]. As a final step in our model development, we use the seven-parameter solution obtained above to seed a nonlinear optimization function with cost function $\sum_{i=1}^{45}(\log(\tilde{P}))^2$. The values for the seven parameters changed negligibly, which we hypothesize is due to the robustness of using the median BET values for each configuration during the initial model fitting.

Our final proposed model is

$$W = \begin{bmatrix} 1.5\text{e}13 & 0 & 0 & 0 & 0 & 0 \\ 0 & 2.2\text{e}13 & 4.8\text{e}13 & 0 & 0 & 0 \\ 0 & 4.8\text{e}13 & 2.2\text{e}13 & -1.2\text{e}15 & 0 & 0 \\ 0 & 0 & -1.2\text{e}15 & 2.0\text{e}16 & 2.0\text{e}15 & 0 \\ 0 & 0 & 0 & 2.0\text{e}15 & 7.8\text{e}13 & 0 \\ 0 & 0 & 0 & 0 & 0 & 7.8\text{e}13 \end{bmatrix} \tag{4}$$

where the upper-left 3×3 block has units N^{-2}, the lower-right 3×3 block has units $\text{N}^{-2}\cdot\text{m}^{-2}$, and the off-diagonal 3×3 blocks have units $\text{N}^{-2}\cdot\text{m}^{-1}$. Recall that this W is for the particular stylus in our experiment, excited at 108 Hz.

Because the dimensional-reduction model we have found requires seven parameters, but was fit using 45 data points (which does not meet the 10-to-1 rule of thumb to avoid the risk of overfitting), we want to explicitly verify that our model is not overfitted. Figure 5 shows the evolution of the individual W_{ij} terms and MSE (for all 45 data points) using a model that was trained using various n values, reducing from $n = 45$ down to $n = 21$. For a given n, we train the parameters in W with the bottom n configurations listed in the table of Fig. 3; this choice was made because configurations lower in that table are increasingly richer at exciting multiple parameters in W. For MSE, in addition to our proposed seven-parameter W, we also show the full 19-parameter W, as well as a three-parameter diagonal W. This diagonal W is a naive approach that assumes orthogonality between all six principal components (i.e., no coupling between them), with $W_{11} = W_{22} = W_{33}$ (consistent with the DFT321 method) and with $W_{55} = W_{66}$ (consistent with our prior results [13]), which results in three independent parameters in total. For our seven-parameter model, there is no evidence of overfitting: the MSE values are insensitive to n, and the W values are undergoing small relative changes. There is also no evidence of overfitting with the three-parameter model, as expected. This cannot be said of the 19-parameter model, which has an MSE value that is still undergoing substantial changes with the addition of new training data. We can also see that our recommended seven-parameter model has a substantially reduced MSE compared to the three-parameter model.

Figure 6 shows the results of our model in (4) applied to the complete data set gathered in Section II, shown as a box-whisker plot. We report the predicted normalized skin-absorbed power in a log-base-10 scale, since our cutaneous system perceives vibrotactile stimuli in this scale based on Stevens' power law [24]. We see qualitatively that the model does a good job of capturing the thresholds obtained across configurations, with inter- and intrasubject variance remaining, which is unavoidable for any one-size-fits-all model.

IV. Discussion

In our prior study that considered each of the six principal components generated at the HIP independently (i.e., one at a time) [13], which used an entirely different human-subjects data set, we observed a number of interesting features that are also present in this data. First, a major conclusion of [13] is that the little-used τ_x stimulus channel (i.e., torque about the axis of the stylus) results in very large relative stimulus intensity. Here, we found a W_{44} that is approximately 260 times larger than W_{55} and W_{66}, confirming that result. Second, in [13], at a frequency of 108 Hz, we observed a blip in the data that suggested that subjects were slightly less sensitive to f_x (i.e., force along the axis of the stylus) than to forces orthogonal to the stylus, even though they were approximately equally sensitive at other frequencies near 108 Hz. At the time, we conjectured that this result was a statistical anomaly. However, our W_{11} value being just 68% of our W_{22} and W_{33} values seems to support this prior result.

For a haptic device that is only capable of rendering forces, our results suggest that an efficient way to render a vibrotactile signal is to superimpose an f_y signal in phase with an f_z signal. Our results suggest that an efficient way to render a vibrotactile signal to a haptic stylus when using a 6D haptic interface is to superimpose a τ_x signal in phase with a τ_y signal (or simply use only a τ_x signal). This is fortuitous considering that quasistatic kinesthetic haptic display typically relies

almost exclusively on rendering of forces at the HIP (e.g., friction, surface normals), leaving torque channels underutilized in 6D haptic interfaces. However, care should be taken when drawing any such conclusions, because knowledge of the maximum forces and torques that can be rendered with a given haptic interface is required in order to fully determine the most efficient ways of rendering vibrotactile sensations.

When attaching a dedicated vibrotactile actuator to a haptic stylus, our results suggest that the actuator should be attached such that vibrations occur orthogonal to the axis of the stylus; this result is consistent with our result in [13]. If possible, the actuator should be attached such that the vibrations occur in the y-z direction when the user holds the stylus, although this latter requirement may be difficult to enforce if the user is allowed to roll the stylus about its axis.

Our results suggest that only three coupling terms are statistically significant: f_z with τ_x, τ_x with τ_y, and f_y with f_z. When beginning this study, it was our conjecture that we would find a coupling of f_y with τ_z, since each of these tend to cause similar motions of the stylus within the grasp (at least quasistatically). Similarly, it was our conjecture that we would find a coupling of f_z with τ_y. However, this study did not find a significant coupling on the terms that we expected based on these simplified quasistatic assumptions.

We must note that our results are not perfectly in line with the assumptions of DFT321, which effectively assumes $W_{11} = W_{22} = W_{33}$ with no coupling terms between force components. The results of our prior study [13] suggest that W_{11} is only different (slightly smaller) than $W_{22} = W_{33}$ for a relatively limited set of frequencies. It is unclear to us why the coupling term has not been identified previously. In any case, when only considering forces at the HIP, using DFT321 would only lead to small errors, even in light of our results.

It must be noted that the W matrix that we found is only for signals at 108 Hz, for our specific stylus. In general, we would need to find W over a range of frequencies of interest, such that each parameter in W would be a function of frequency, and this process would need to be completed for each new stylus, following the methodology outlined in this article. However, to estimate W with seven independent parameters, we found that only 17 configurations were sufficient to train the model, which is well below the 70 that would be suggested by the 10-to-1 rule of thumb. It may also be possible to calibrate the W parameter functions using a reduced set of frequencies and/or using stylus properties, but this is left as an open problem.

REFERENCES

[1] K. O. Johnson, "The roles and functions of cutaneous mechanoreceptors," *Curr. Opin. Neurobiol.*, vol. 11, no. 4, pp. 455–461, 2001.

[2] L. A. Jones and S. J. Lederman, *Human Hand Function*. London, U.K.: Oxford Univ. Press, 2006.

[3] S. J. Lederman and R. L. Klatzky, "Haptic perception: A tutorial," *Atten. Percept. Psycho.*, vol. 71, no. 7, pp. 1439–1459, 2009.

[4] A. M. Okamura, M. R. Cutkosky, and J. T. Dennerlein, "Reality-based models for vibration feedback in virtual environments," *IEEE/ASME Trans. Mechatronics*, vol. 6, no. 3, pp. 245–252, Sep. 2001.

[5] K. J. Kuchenbecker, J. Fiene, and G. Niemeyer, "Improving contact realism through event-based haptic feedback," *IEEE Trans. Visualization Comput. Graph.*, vol. 12, no. 2, pp. 219–230, Mar./Apr. 2006.

[6] J. R. Napier, "The prehensile movements of the human hand," *Bone Joint J.*, vol. 38, no. 4, pp. 902–913, 1956.

[7] S. Choi and K. J. Kuchenbecker, "Vibrotactile display: Perception, technology, and applications," *Proc. IEEE*, vol. 101, no. 9, pp. 2093–2104, Sep. 2013.

[8] J. Bell, S. Bolanowski, and M. H. Holmes, "The structure and function of pacinian corpuscles: A review," *Prog. Neurobiol.*, vol. 42, no. 1, pp. 79–128, 1994.

[9] H. Culbertson, J. Unwin, and K. J. Kuchenbecker, "Modeling and rendering realistic textures from unconstrained tool-surface interactions," *IEEE Trans. Haptics*, vol. 7, no. 3, pp. 381–393, Jul.–Sep. 2014.

[10] H. Culbertson, J. J. L. Delgado, and K. J. Kuchenbecker, "One hundred data-driven haptic texture models and open-source methods for rendering on 3D objects," in *Proc. IEEE Haptics Symp.*, 2014, pp. 319–325.

[11] N. Landin, J. M. Romano, W. McMahan, and K. J. Kuchenbecker, "Dimensional reduction of high-frequency accelerations for haptic rendering," in *Proc. Int. Conf. Human Haptic Sens. Touch Enabled Comput. Appl.*, 2010, pp. 79–86.

[12] G. Park and K. J. Kuchenbecker, "Objective and subjective assessment of algorithms for reducing three-axis vibrations to one-axis vibrations," in *Proc. IEEE World Haptics Conf.*, 2019, pp. 467–472.

[13] R. Zhang, A. J. Boyles, and J. J. Abbott, "Six principal modes of vibrotactile display via stylus," in *Proc. IEEE Haptics Symp.*, 2018, pp. 313–318.

[14] B. Hannaford and A. M. Okamura, "Haptics," in *Springer Handbook of Robotics*. Berlin, Germany: Springer, 2016, ch. 30, pp. 1063–1084.

[15] J. J. Abbott, E. Diller, and A. J. Petruska, "Magnetic methods in robotics," *Annu. Rev. Cont. Robot. Autom.*, vol. 3, pp. 2.1–2.34, 2020.

[16] H.-Y. Yao, D. Grant, and M. Cruz, "Perceived vibration strength in mobile devices: The effect of weight and frequency," *IEEE Trans. Haptics*, vol. 3, no. 1, pp. 56–62, Jan.–Mar. 2009.

[17] A. J. Petruska and J. J. Abbott, "Omnimagnet: An omnidirectional electromagnet for controlled dipole-field generation," *IEEE Trans. Magn.*, vol. 50, no. 7, 2014, Art. no. 8400810.

[18] H. R. Dinse, P. Ragert, B. Pleger, P. Schwenkreis, and M. Tegenthoff, "Pharmacological modulation of perceptual learning and associated cortical reorganization," *Science*, vol. 301, no. 5629, pp. 91–94, 2003.

[19] T. N. Cornsweet, "The staircase-method in psychophysics," *Amer. J. Psychol.*, vol. 75, no. 3, pp. 485–491, 1962.

[20] G. A. Gescheider, *Psychophysics: The Fundamentals*. Psychology Press, Mahwah, New Jersey, 2013.

[21] I. Hwang, J. Seo, M. Kim, and S. Choi, "Vibrotactile perceived intensity for mobile devices as a function of direction, amplitude, and frequency," *IEEE Trans. Haptics*, vol. 6, no. 3, pp. 352–362, Jul.–Sep. 2013.

[22] R. D. Howe and M. R. Cutkosky, "Sensing skin acceleration for slip and texture perception," in *Proc. IEEE Int. Conf. Robot. Autom.*, 1989, pp. 145–150.

[23] N. Zamani and H. Culbertson, "Effects of dental glove thickness on tactile perception through a tool," in *Proc. IEEE World Haptics Conf.*, 2019, pp. 187–192.

[24] S. S. Stevens, "On the psychophysical law." *Psychol. Rev.*, vol. 64, no. 3, pp. 153–181, 1957.